A quantitative proteomic approach to highlight Phragmites sp. adaptation mechanisms to chemical stress induced by a textile dyeing pollutant

R.A. Ferreira [a,1], C. Roma-Rodrigues [b,1,2], L.C. Davies
a,c,1,3 Sá-Correia [b,c], S. Martins-Dias [ac-* *
[a] Centre for Natural Resources and the Environment (CERENA), Instituto Superior Técnico, Universidade de Lisboa, Av. Rovisco Pais, 1049-001 Lisboa, Portugal [b] Institute for Bioengineering and Biosciences, Instituto Superior Técnico, Universidade de Lisboa, Av. Rovisco Pais, 1049-001 Lisboa, Portugal [c] Department of Bioengineering, Instituto Superior Técnico, Universidade de Lisboa, Av. Rovisco Pais, 1049-001 Lisboa, Portugal

HIGHLIGHTS

- Phragmites sp . early response to oxida- tive stress and adaptation was studied.
- Phragmites leaf proteome alterations due to AO7 were followed up to 24.25 h.
- Signalling was promptly activated, three identified proteins abundance increased.
- Carbohydrate metabolism boost the energy flows due to photosynthesis inhibition.

GRAPHICAL ABSTRACT

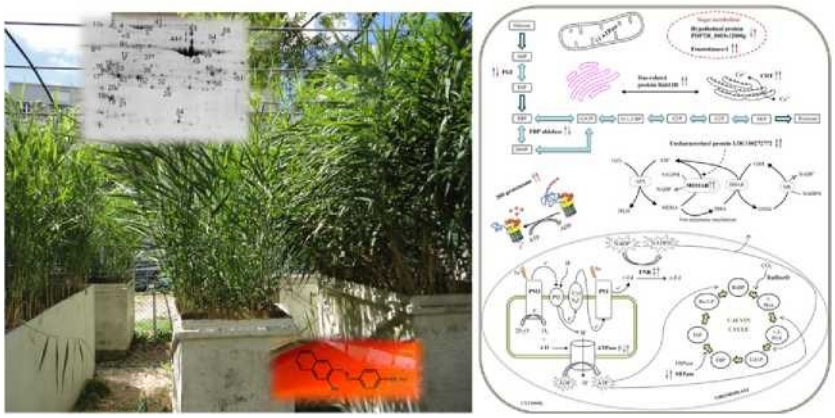

abstract
Phragmites sp. is present worldwide in treatment wetlands though the mechanisms involved in the phytoremediation remain unclear. In this study a quantitative proteomic approach was used to study the prompt response and adaptation of Phragmites to the textile dyeing pollutant, Acid Orange 7 (AO7). Previously, it was demonstrated that AO7 could be successfully removed from wastewater and mineralized in a constructed wet- land planted with Phragmites sp. This azo dye is readily taken up by roots and transported to the plant aerial part by the xylem. Phragmites leaf samples were collected from a pilot scale vertical flow constructed wetland after 0.25, 3.25 and 24.25 h exposure to AO7 (400 mg L^{-1}) immediately after a watering cycle used as control. Leaf soluble protein extraction yielded an average of 1560 proteins in a broad pI range (pH 3-10) by two-dimensional gel electrophoresis. A time course comparative analysis of leaf proteome revealed that 40 proteins had a differential abundance compared to control (p b 0.05) within a 3.25 h period. After 24.25 h in contact with AO7, leaf proteome was similar to control. Adaptation to AO7 involved proteins related with cellular signal- ling (calreticulin, Ras-related protein Rab11D and 20S proteasome), energy production and conversion (adeno- sine triphosphate synthase beta subunit) carbohydrate transport and metabolism (phosphoglucose isomerase, fructose-bisphosphate aldolase, monodehydroascorbate reductase, frutockinase-1 and Hypothetical protein POPTR_0003s12000g and the Uncharacterized protein LOC100272772) and photosynthesis (sedoheptulose- 1,7-bisphosphatase and ferredoxin-$NADP^+$ reductase). Therefore, the quantitative proteomic approach used in this work indicates that mechanisms associated with stress cell signalling, energy production, carbohydrate transport and metabolism as well as proteins related with photosynthesis are key players in the initial chemical stress response in the phytoremediation process of AO7.

Keywords:
Acid Orange 7
Azo dyes
Constructed wetlands

Photosynthesis
Phytoremediation
Signalling

1. Introduction

Textile industry plays a major role in the economy of many countries around the world, where a large amount of wastewaters contaminated with unfixed dyes are being produced (Ghaly et al., 2014). Dyes, of which the majority are azo dyes designed to resist to abiotic and biotic degradation remain nearly unchanged throughout conventional waste- water treatment processes contaminating the receiving water bodies (Banat et al., 1996; Sanromán et al., 2004). Moreover, large quantities of untreated textile dyeing wastewaters are being discharged daily by small size companies in low-income regions to the nearest water stream, mostly due to the lack of affordable treatment technologies. Whereas veg- etation lining the banks survives to the contaminated waters, the mam- malian health is undermined by dermal exposure and absorption of azo dyes metabolites produced by skin microorganisms or via ingestion, as liver enzymes and intestinal flora are also able to split azo dyes into aro- matic amines that can be more toxic than the parent molecule (Bhaskar et al., 2003; Chung et al., 1992). Prevalent vegetation in constructed wet- lands (CWs) consists of macrophytes (e.g. Phragmites sp.) that easily adapt to the presence of pollutants. Besides plants ability to alter the chemical form of contaminants by changing the soil environment (e.g., pH and redox potential) around the roots (Verkleij et al., 2009) and via the release of exudates and oxygen (Hinsinger et al., 2009) pro- moting microbial growth they also play a role in detoxification pathways of diverse xenobiotics (Schwitzguébel et al., 2011). The uptake of xenobi- otics by plants depends on root-water-soil interactions. The translocation from plant roots to xylem is considered optimal for those compounds that are only slightly hydrophobic (0.5 b Log Kow b 3.5). These compounds seemed to enter the xylem faster than the soil and rhizosphere microflora can degrade them (Barac et al., 2004). Thus, under normal circumstances, plants have to metabolise endogenous and exogenous compounds that may lead to a sudden increase in plant endogenous intracellular reactive oxygen species (ROS) content. While, the major ROS generation sites are considered the reaction centres of photosystems I and II in chloro- plasts, under stress conditions the disruption of the electron transport systems linked to mitochondrial and plasma membranes also leads to an increase in ROS production (Demidchik, 2015).

Phragmites are ubiquitous species belonging to the Poaceae family found in wetland areas and commonly used in CW treatment systems, being effective in treating domestic, agricultural and industrial waste- waters (Haberl et al., 2003; Wu et al., 2015). Phragmites has been proved to be an excellent plant for use in CWs also due to its phyto- treatment capacity of textile azo dyes contaminated wastewaters (Carias et al., 2008; Davies et al., 2009; Davies et al., 2006; Ferreira et al., 2014). Phragmites sp. prompt response to the chemical stress im- posed by Direct Red 81 (a di-azo dye) revealed the importance of the photosynthetic pigments involvement in early signalling, the synergy between the antioxidant enzymes and the ascorbate-glutathione cycle, and the activation of the detoxification system (Ferreira et al., 2014). Indeed the expression of genes coding for ROS scavenging en- zymes were found to be stimulated in Phragmites root and leaf tissues after plant exposure to the azo dye Acid Orange 7 (AO7) and the plant detoxification system was simultaneously activated (Davies et al., 2009).

How vegetation adapts to pollutants and its role in textile dyeing wastewaters decontamination is a crucial research in order to enable a proper selection of vegetation for treatment (constructed) wetlands and its design and operation. These engineered wetlands are affordable almost anywhere.

In the present work, AO7 was selected as an azo dye model mol- ecule. AO7 chemical properties (pKa of 8.2; Log Kow of 0.56) allow for plant uptake and transport by xylem to the aerial part of the plant while it is not expected to be excreted by phloem (Collins et al., 2006). Therefore, it may be metabolised in Phragmites leaf tis- sues leading to AO7 high removal efficiencies (Davies et al., 2006). To get new insights into the global mechanisms underlying Phragmites response to azo dyes, the variations occurring in soluble leaf proteins abundance after exposure to AO7 were followed using a quantitative proteomic approach. Proteomics studies significantly contributed to unravel the relationships between protein abundance and plant stress adaptation for other plant species (for review see Kosová et al., 2011).

2. Materials and methods

2.1. Sample preparation

A pilot scale vertical flow constructed wetland (VFCW) (0.96 m^2 x 0.7 m) planted with Phragmites sp. in a sandy-clay soil was pulse-fed every 3 h for 15 min, ca. 15 L. The feeding of the VFCW was changed from tap water to an aqueous solution of AO7 at 400 mg L^{-1} in three separate occasions in different seasons (biological triplicates) (Davies et al., 2010). Leaves were collected at the end of a last water pulse (control) and after the pulse-fed period of the 1st, 2nd and 8th

(0.25h,3.25hand24.25h)AO7feedingcycle.Leafsampleswerecollect- ed randomly and immediately frozen in liquid nitrogen, as previously re- ported (Ferreira et al., 2014), and reduced to a fine powder using a 6770 SPEX SamplePrep Freezer/Mill (-196 °C). The grinding was done in 2 cycles of 10 min at maximum frequency, between grinding cycles sam- ples were cooled for 2 min to achieve optimum brittleness again; 100 mg of powder portions were transferred intosterilemicrotubes,suspended in 1 mL of PBS (0.01 M, pH 7.4) with a protease inhibitor cocktail (10% (v/v); cOmplete, Roche) and incubated in a rotary shaker for 1 h at 20 °C.

Cell wall and debris were removed by centrifuging (20,800g; 15 min) and the supernatant was filtered using sterile low protein- binding syringe filters (0.2 |im). Ribulose-1,5-bisphosphate carboxyl- ase/oxygenase (RuBisCO) was removed with IgY antibodies cross- linked to microbeads (Seppro® RuBisCO Spin Column, Sigma-Aldrich). To the remaining proteins, (3-mercaptoethanol was added to a final con- centration of 2%, in solution. Total protein content was determined with 2-D Quant Kit (GE Healthcare) according to the manufacturer instruc- tions. Aliquots of 25 jwg of protein were precipitated using the 2-D

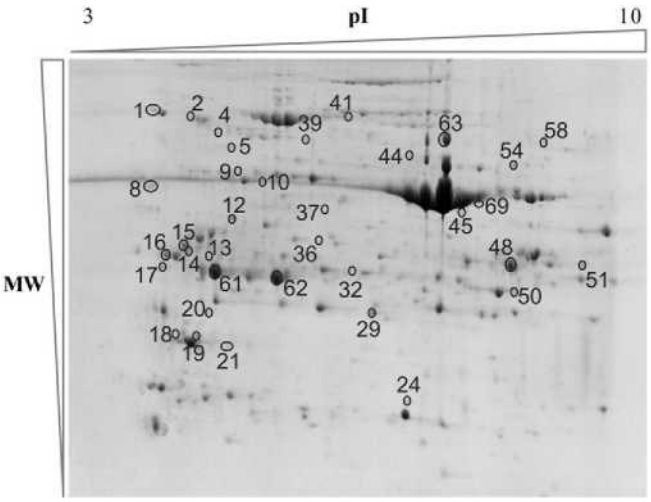

Fig. 1. Representative proteome map of Phragmites sp. leaf proteins. Proteins were separated by 2-DE (pI between 3 and 10; SDS-PAGE 12%) and visualized by staining with Coomassie Blue R-350. The identified protein spots are numbered as in Table 1.pI: isoelectric point; MW: molecular weight.

Clean-Up Kit (GE Healthcare) to remove isoelectric focusing (IEF) inter- fering compounds according to the manufacturer instructions. Samples were kept up to two weeks at - 20 °C.

2.2. Two-dimensional gel electrophoresis

Before IEF, samples were centrifuged (12,000g; 10 min) and pelleted proteins were solubilized in 100 pL IEF buffer (9 M urea, 2% w/v 3-((3- cholamidopropyl) dimethylammonio)-1-propanesulfonate, 0.5% w/v Pharmalytes 3-10,15 mM 1,4-dithiothreitol and traces ofbromophenol blue). Proteins were quantified and each analytical sample was pre- pared byadjusting protein concentration to 100 pgin80pLofIEFbuffer. A two-dimensional gel electrophoresis (2-DE; 12% polyacrylamide gel) procedure was then carried out (Roma-Rodrigues et al., 2010).Atotal of 12 gels were run, corresponding to 3 gels for each one of the three dif- ferent experimental conditions and control. A preparative sample was run in parallel with the samples under study (24.25 h samples were ex- cluded). This sample was prepared by pooling together 400 pgofpro- tein extract obtained from each different biological sample under study. The resulting preparative gel was stained with Coomassie Blue R-350 (Santos et al., 2004).

2.3. Analysis of protein abundance levels

Analytical gel images were analysed with Progenesis Samespots software package (Nonlinear Dynamics, Newcastle, UK), essentially as described before (Roma-Rodrigues et al., 2010; Santos and Sa-Correia, 2009). Protein spots were identified using the automatic spot detection algorithm. Individual spot volumes were normalized against total spot volumes ofthe respective gel. Spots that showed evidence of saturation were not further analysed. The normalized volume averages of each protein spot were compared using one-way ANOVA between-group test. Statistically significant spots were considered at p b 0.05 and Progenesis Power score N 70%.

Progenesis Samespots software was also used in Principal Compo- nent Analysis (PCA) of 2-DE gel protein patterns among control and AO7 conditions.

2.4. Identification of proteins by peptide mass fingerprinting

The identification of protein spots of interest was performed byPep- tide Mass fingerprint using MALDI-

TOF/TOF tandem mass spectrometry (MS/MS) in the proteomic unit at Centro Nacional de Investigaciones Cardiovasculares Carlos III, Madrid, Spain (CNIC Foundation), as a paid service.

2.4.1. In-gel trypsin digestion

Protein spots were excised from the preparative gel manually and transferred to pierced V-bottom 96-well polypropylene microplates (Bruker Daltonik) loaded with ultrapure water. The samples were digested automatically using a Proteineer DP robot (Bruker Daltonik) under the control ofdpControl 1.2 software (Bruker Daltonik) according to the protocol of Shevchenko et al. (2006) with the modifications of Madeira et al. (2011) and other minor variations: modified porcine trypsin at a final concentration of8 ngpL^{-1} in 50 mM ammoniumbicar- bonate was added to the dry gel pieces and the digestion proceeded at 37 °C for 8 h; finally, 0.5% trifluoroacetic acid was added for peptide extraction, and the resulting digestion solutions transferred by centrifu- gation to V-bottom 96-well polypropylene microplates (Greiner Bio- One).

2.4.2. Mass spectrometry

MALDI samples were prepared by mixing equal volumes of the above digestion solution and a matrix solution composed of a-cyano- 4-hydroxycinnamic acid in 50% aqueous acetonitrile and 0.25% trifluoroacetic acid. This mixture was deposited onto a 600 pm

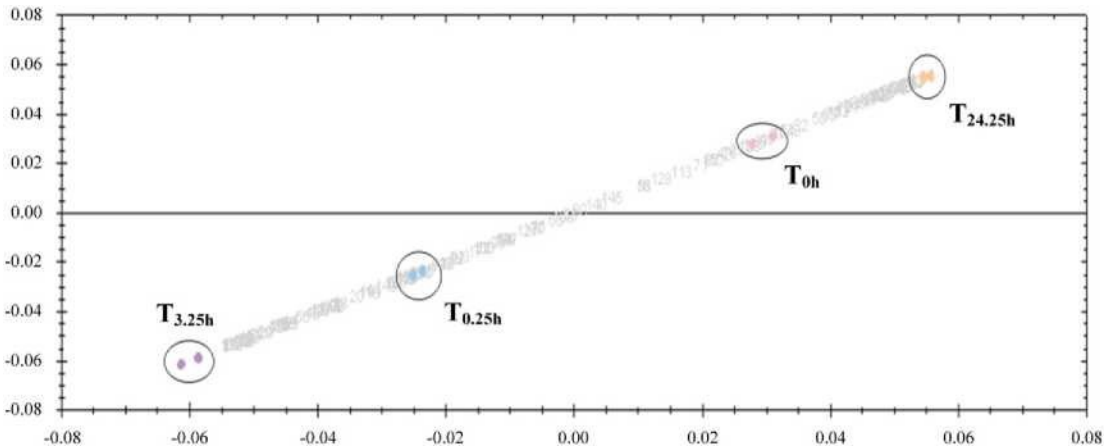

Fig. 2. One-dimensional Principal Component Analysis (PCA) of protein patterns in 2-DE gels. The PCA used first principal component for analysis of the gels prepared from Phragmites leaves collected from a VFCW at the end of a last water pulse (T0) and at the end of the 1st (T0.25h), 2nd (T3.25h) and 8th (T24.25h) feeding period of AO7 (400 mg L^{-1}). Spots inside circles represent each gel prepared for the indicated condition. The grey line represents the clustering of the proteins detected in the corresponding 2-DE gels. Both axes correspond to PCA 1.

Table 1
Identification of *Phragmites sp.* leaf proteins and relative alterations after 0.25 and 3.25h exposure to Acid Orange 7 (AO7 at 400 mg L^{-1}) as compared to control (water). *Phragmites* leaves were collected from a pilot vertical flow constructed wetland pulse-fed every 3 h for 15 min. PM: number of peptides matched; SC: protein sequence coverage.

Functional classification	Spot ID[a]	Matched protein name (Submitted name[b])	Taxonomy	Accession code[c]	Score[d]	PM	SC (%)	Theoretical		Fold[e]		ANOVA / power score (%)[f]
								MW (Da)	pI	$T_{0.25h}/T_0$	$T_{3.25h}/T_0$	
Cellular processes and signalling:												
Post-translational modification, protein turnover and chaperones	1	Os12g0244100 protein (70 kDa heat shock protein)	*Oryza sativa subsp. japonica*	NP_001066486	124	10	21	74269	5.11	1	1	
	2	PREDICTED: probable mediator of RNA polymerase II transcription subunit 37c	*Zea mays*	XP_008660826	182	12	26	71447	5.13	1	1	
	8	Calreticulin2 precursor (Calcium-binding protein)	*Zea mays*	CAA86728	106	7	18	48154	4.48	1.4	1.4	1.48E−02 / 92
	24	Maize 20S Proteasome alpha subunit (Proteasome subunit alpha type)	*Zea mays*	NP_001105138	126	7	32	27500	6.10	1.4	1.7	3.73E−02 / 70
Intracellular trafficking, secretion and vesicular transport	4	PREDICTED: Ras-related protein Rab11D	*Fragaria vesca subsp. Vesca*	XP_004288173	78	5	27	24614	8.44	2.2	1.1	1.75E−02 / 89
Metabolism:												
Energy production and conversion	9	Hypothetical protein PHAVU_007G034800g (ATP synthase subunit beta)	*Phaseolus vulgaris*	XP_007142995	96	8	19	59811	5.77	0.8	0.7	1.61E−02 / 91
	10	ATP synthase beta subunit, partial, plastid	*Phragmites australis*	ABR67207	137	9	30	51107	5.20	0.8	1.2	3.06E−02 / 76
	18	Pyrophosphate-energized proton pump1	*Zea mays*	NP_001140851	129	8	26	31731	5.79	1	1	
	39	Hypothetical protein OsJ_17383 (Malic enzyme)	*Oryza sativa subsp. japonica*	EEE62580	74	6	11	59086	5.67	1	1	
Carbohydrate transport and metabolism	12	PREDICTED: Monodehydroascorbate reductase	*Setaria italica*	XP_004956201	104	7	18	46768	5.81	1.6	1.3	5.55E−03 / 99
	14	Hypothetical protein POPTR_0003s12000g	*Populus trichocarpa*	XP_002303557	71	5	17	34169	6.9	0.6	1.1	1.65E−02 / 90
	17	PREDICTED: Fructokinase-1	*Setaria italica*	Si002240m.g	170	10	37	34797	5.05	1.4	1.2	3.65E−02 / 71
	19	Putative glyoxalase I	*Oryza sativa subsp. japonica*	BAD28547	68	6	20	32394	5.82	1	1	
	36	Hypothetical protein, partial (Phosphoglycerate kinase)	*Zoysia matrella*	AIN39803	79	4	16	30988	8.65	1	1	
	45	Uncharacterized protein LOC100272772	*Zea mays*	NP_001140697	96	7	17	54074	8.65	1	1.7	2.70E−02 / 79
	51	PREDICTED: fructose-bisphosphate aldolase, cytoplasmic isozyme 1-like	*Setaria italica*	XP_004965915	91	6	18	38331	6.78	1.9	0.6	2.85E−02 / 78
	54	Glucose-6-phosphate isomerase, cytosolic (Phosphoglucose isomerase)	*Zea mays*	P49105	100	8	17	62483	6.96	1.6	0.8	4.16E−02 / 70

(continued on next page)

Table 1 (*continued*)

Functional classification	Spot ID[a]	Matched protein name (Submitted name[b])	Taxonomy	Accession code[c]	Score[d]	PM	SC (%)	Theoretical		Fold[e]		ANOVA / power score (%)[f]
								MW (Da)	pI	$T_{0.25h}/T_0$	$T_{3.25h}/T_0$	
	61	PREDICTED: Fructose-bisphosphate aldolase, chloroplastic	*Brachypodium distachyon*	XP_003577785	109	8	17	42189	6.26	1	1	
	62	Fructose-bisphosphate aldolase	*Zea mays*	ACG36798	85	6	14	41924	7.63	1	1	
Amino acid transport and metabolism	41	5-methyltetrahydropteroyltriglutamate–homocysteine methyltransferase 1 (Cobalamin-independent methionine synthase)	*Oryza sativa subsp. japonica*	Q2QLY5	134	11	19	84874	5.93	1	1	
Photosynthesis	16	Sedoheptulose-1,7-bisphosphatase, chloroplastic	*Triticum urartu*	EMS67709	100	8	23	40102	5.74	0.7	1.2	2.69E−02 / 79
	21	PREDICTED: oxygen-evolving enhancer protein 1, chloroplastic	*Setaria italica*	XP_004968772	70	5	21	35111	5.74	1	1	
	29	Hypothetical protein SORBIDRAFT_03g046340 (Ferredoxin-NADP$^+$ reductase)	*Sorghum bicolor*	XP_002459129	88	9	23	41311	6.50	1	1.5	2.94E−02 / 77
	44	Ribulose-1,5-bisphosphate carboxylase/oxygenase large subunit, partial, chloroplast	*Australopyrum velutinum*	AAX44944	198	15	32	52228	6.23	1	1	
	63				222	16	32			1	1	
	69		*Veronica officinalis*	AEK34549	119	8	18	48602	6.33	1	1	
Inorganic ion transport and metabolism	58	PREDICTED: catalase-1	*Brachypodium distachyon*	XP_003558892	110	10	25	56996	6.78	1	1	
Information storage and processing:												
RNA processing and modification	13	Predicted protein (PHYPADRAFT_188860)	*Physcomitrella patens subsp. patens*	XP_001770408	73	5	54	17963	5.84	1	1	
Chromatin structure and dynamics	32	Hypothetical protein AMTR_s00003p00196050	*Amborella trichopoda*	ERN03255	76	5	26	22388	6.36	0.7	0.5	1.97E−02 / 87
Uncharacterized proteins:												
	5	Os12g0420200 protein (RNA binding protein, putative, expressed)	*Oryza sativa subsp. japonica*	NP_001066657	95	8	27	41621	8.59	1	1	
	50				105	8	25			1	1	
	15	Hypothetical protein JCGZ_05247	*Jatropha curcas*	JCGZ_05247	71	4	21	21733	7.71	1	1	
	20	BnaC03g38320D protein	*Brassica napus*	CDX75749	72	7	9	124610	5.81	0.7	0.5	4.63E−02 / 70
	37	Hypothetical protein L484_007757	*Morus notabilis*	XP_010099394	75	6	17	40892	6.92	1	1	
	48	Predicted protein	*Hordeum vulgare var. distichum*	BAJ99064	118	10	25	42269	6.41	1	1	

[a] Consistent with the spot number of Fig. 1.
[b] Submitted and/or recommended protein name in the UniProtKB database (if different from the matched protein name deposited in the NCBInr and/or SwissProt databases).
[c] Accession number of the matched protein in the NCBInr and/or SwissProt databases.
[d] MASCOT score; protein scores greater than 68 are significant ($p < 0.05$).
[e] Fold changes correspond to the ratio values of normalized protein spots in 2-DE gels obtained at the end of the 1st ($T_{0.25\ h}$) and 2nd ($T_{3.25\ h}$) pulse feeding period cycle of AO7 (400 mg L^{-1}) in relation to control (T_0; pulse feeding with water). Alterations were considered statistically different at $p < 0.05$.
[f] Values equal or below 0.05 and with Progenesis Power Score higher than 70% were considered to ensure high statistical confidence of differential expression.

AnchorChip prestructured MALDI probe (Bruker Daltonik) (Schuerenbeg et al., 2000) and allowed to dry at room temperature. Samples were automatically analysed in an Ultraflex MALDI-TOF/TOF mass spectrometer (Bruker Daltonik) (Suckau et al., 2003) with an au- tomated analysis loop using internal mass calibration, under the control of flexControl 2.2 software (Bruker Daltonik). In a first step, the MALDI- MS spectra were acquired by averaging 300 individual spectra in the positive ion reflector mode at 50 Hz laser frequency in a mass range from 800 to 4000 Da. Internal calibration of MALDI-MS mass spectra was performed using two trypsin autolysis ions with m/z = 842.510 and m/z = 2211.105. In a second step, precursor ions exceeding a threshold signal-to-noise ratio in the MALDI-MS mass spectrum were subject to fragment ion analysis in the tandem (MS/MS) mode. Precur- sors were accelerated to 8 kV and selected in a timed ion gate. Fragment ions generated by laser-induced decomposition of the precursor were further accelerated by 19 kV in the LIFT cell and their masses were analysed after passing the ion reflector to average 1000 spectra. MALDI-MS/MS calibrations were performed with fragment ion spectra obtained for the proton adducts of a peptide mixture covering the 800-3200 m/z region. MALDI-MS and MS/MS spectra were manually inspected in detail and reacquired, recalibrated and/or relabelled when necessary.

2.4.3. Database searching

MALDI-MS and MS/MS data were combined through the BioTools 3.0 program (Bruker Daltonik) to search a non-redundant protein data- base, NCBInr 20151125 (77,306,371 sequences; 28,104,191,422 resi- dues) or SwissProt 2015_11 (549,832 sequences; 196,078,138 residues), using MASCOT software (http://www.matrixscience.com; Matrix Science, London, UK). Search parameters were setas: taxonomy, Viridiplantae (Green Plants); proteolytic enzyme, trypsin; allow up to one missed cleavages; fixed modifications, carbamidomethyl (C); vari- able modifications, oxidation (M); monoisotopic peptide mass (NH^+); peptide mass tolerance ±50 ppm; MS/MS tolerance ±0.5 Da. Only sig- nificant hits, as defined by the MASCOT probability analysis (p b 0.05), were considered in subsequent data analyses. The protein identifica- tions were validated according to the following criteria: score N68, low- est expect, at least four peptide matches and at least 10% sequence coverage.

The protein species were functionally categorized using UniProtKB (Universal Protein Resource Knowledgebase; http://www.uniprot. org), EggNOG v4.5 (Evolutionary Genealogy of Genes: Non-supervised Orthologous Groups;http://eggnogdb.embl.de) and KEGG (Kyoto Ency- clopedia of Genes and Genomes; http://www.kegg.jp) combined with manual analysis.

3. Results and discussion

3.1. Protein spots separation, image analysis and protein species identification

The objective of this studywas to elucidate changes in protein abun- danceassociated withprogressionofexposuretimeofPhragmitesplants to AO7 in a time course of24h byanalyzing leaf soluble proteome via 2- DE. To that purpose a pilot VFCW planted with Phragmites sp. was pulse fed every3 hfor15min withAO7at400 mgL^{-1}. Plantleaves were sam- pled immediately after each feeding cycle, as

described in Section 2.1., and processed. Abundance of several proteins was altered depending upon the contact time and MALDI-TOF/TOF was used to identify a num- ber of these proteins.

Among all 2-DE gels obtained in this proteomic analysis, an average of 1560 proteins with a pI range from pH 3 to pH 10 were separated (Fig. 1). The proteins patterns under the analysed conditions were compared by a one-dimensional PCA (Fig. 2). The 1st (0.25 h) and 2nd (3.25 h) feeding cycles were clustered in the same vicinity of the first principal component, the 8th cycle (24.25 h) was located at the vicinity ofthe control sample. This result suggests higher similaritybetween the control and the 24.25 h protein patterns and hence that major plant ad- aptations to AO7 did occur in the first feeding cycles, consistent with previous observations (Davies et al., 2010). Therefore, only the 0.25 h and 3.25 h samples were considered for further analysis.

Proteins spots were selected for identification based on a prelimi- nary expression analysis of the obtained 2-DE protein patterns using Progenesis SameSpots software. Protein spots excised from the gel were analysed by MS/MS using a peptide mass fingerprint approach. Among the 90 proteins selected for identification, 35 had homology with protein sequences deposited in NCBI and SwissProt databases (Table 1; see also supplementary Table S1). A significant percentage of the protein spots could not be identified (62%)due to the absence ofsig- nificant homologous proteins in databases. The identified proteins presented a high homology with proteins of Zea mays (27%) and Oriza sativa (23%), Fig. 3, but only one protein had high homology with a Phragmites sp. protein (spot 10).

Currently, only about 600 Phragmites sp. gene sequences are avail- able in GenBank, while several of them are still registered as “unnamed protein product”. Therefore, mostofthe proteins whose abundance was found to be modified in response to AO7 had no significant homology with proteins in databases (see supplementary Table S2). However, they seemed to play an important role in the response of Phragmites sp. leaf tissues to the presence of AO7, since their abundance had the most significant alterations ($p < 0.05$), e.g., the abundance of protein spot number 26 (Fig. S1 and supplementary Table S2) increased 5.7 times after 3.25 h.

Moreover, it is not possible to compare the overall results with the proteomic analysis of two Phragmites ecotypes accomplished by Cui et al. (2009) as proteins extraction methodology and pI range under study are different. Even though, some of the proteins linked to photo- synthesis function showed some similarity (spot 16, 21, 29).

A functional characterisation of the 35 identified proteins was established using UniProtKB, EggNOG, KEGG databases and other re- ports in the literature (Table 1). From the identified proteins, 6 (17.1%) had homology with proteins whose function is unknown. The 29 remaining identified proteins were classified into three main orthologous categories: cellular processes and signalling (14.3%), me- tabolism (62.9%) and information storage and processing (5.7%). The functional groups of each main category are presented in Fig. 4. Two functional groups from the metabolism category stand out: 28.6% of proteins are involved in carbohydrate transport and metabolism and 17.1% in photosynthesis.

3.2. Time-dependent alterations of the proteome of Phragmites sp. leaves due to AO7

Significant abundance differences ($p < 0.05$) were denoted in 15 identified proteins and found as AO7 contact time dependent (Table 2). Immediately after the first 15 min in contact with AO7, the content of proteins related to signal transduction pathways like Ras- related protein Rab11D, calreticulin (CRT) and 20S proteasome (20SP) (spot 4, 8 and 24, respectively) increased as compared to control (Tables 1 and 2; Fig. 5).

Other variations were also associated to proteins functional catego- ries denoting a main alteration on those associated with metabolism when exposure time increased from 0.25 h to 3.25 h (Fig. 5). Indeed, it was observed: (a) an increased abundance of the protein adenosine triphosphate (ATP) synthase beta subunit (ATPase (3; spot 10) related to energy production and conversion; of the Hypothetical protein POPTR_0003s12000g (spot 14) and Uncharacterized protein LOC100272772 (spot 45) related to carbohydrate transport and metabolism; and of the sedoheptulose-1,7-bisphosphatase (SBPase; spot 16) and ferredoxin-$NADP^+$ reductase (FNR; spot 29) related to photosynthesis; (b) a decrease in abundance of the proteins fructose-bisphosphate (FBP) aldolase (spot 51) and phosphoglucose

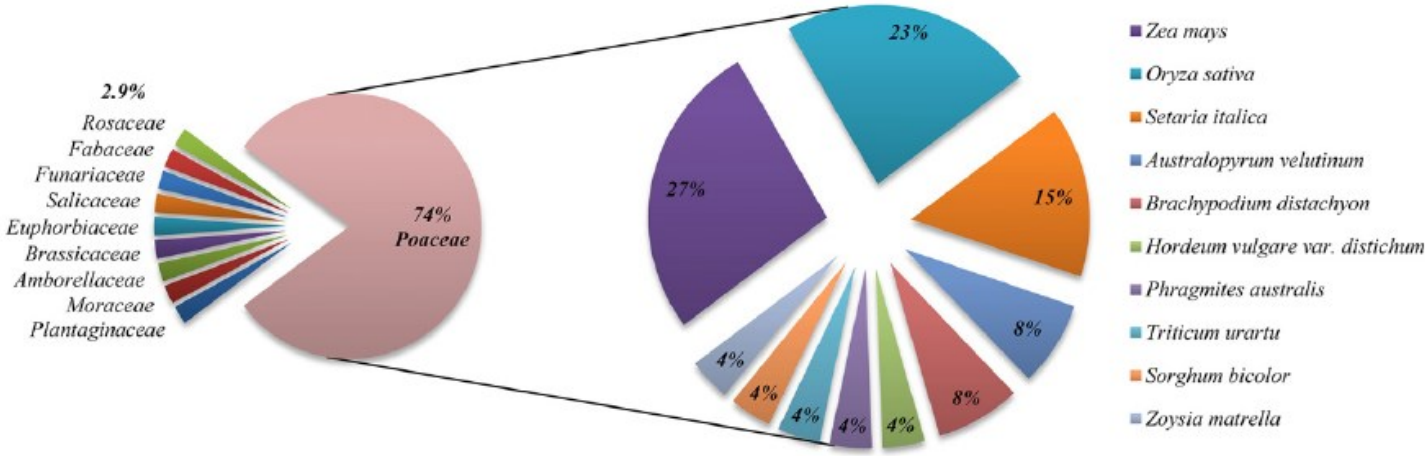

Fig. 3. Taxonomy analysis of the identified Phragmites sp. leaf proteins: taxonomy families (left chart) and taxonomy species of the Poaceae family (right chart; legend follows percent descending order).

isomerase (PGI; spot 54) related to carbohydrate transport and metabolism.

A schematic representation of the chemical stress-induced changes in major metabolic pathways of Phragmites sp. leaves is presented in Fig. 6.

3.2.1. Changes in proteins involved in cellular process and signalling

Since plants use specific messengers (e.g., ROS or the modulated in- tracellular calcium) to regulate their metabolic processes to adapt to minute changes imposed by biotic or abiotic stresses (Garg et al., 2015; Yan et al., 2014) a prompt response to AO7 presence might have occurred. Thus, the rapid increase (at 0.25 h) of abundance of CRT, 20SP alpha subunit and Ras-related protein Rab11D in Phragmites sp. leaves may be part of the complex stress signalling strategy occur- ring in this plant species.

CRT protein is a major calcium-binding molecular chaperone located in the lumen of the endoplasmatic reticulum (Garg et al., 2015) but also outside the endoplasmatic reticulum compartments such as the Golgi apparatus, cytosol, nucleus and cell surface (Qiu et al., 2012). CRT are quality control systems of protein folding machinery promoting correct folding of proteins that enter the secretory pathway and targets misfolded proteins for degradation (Gupta and Tuteja, 2011). They have been implicated in different signalling pathways specific to plants (Agrawal et al., 2002; Heilmann et al., 2001; Komatsu et al., 2007; Sharma et al., 2004).

20SP alpha subunit abundance increased gradually during the course event of Phragmites exposure to AO7. In eukaryotes, the 20SP is the core complex of the 26SP, which degrades ubiquitinated target mol- ecules in an ATP-dependent manner. Protein ubiquitination regulates many processes in eukaryotic cells, varying from cell division through communication/signalling to cell death. In plants, the ubiquitin/protea- some pathway of protein degradation has been implicated in plant responses to internal and external stimuli, comprising phytohormones, abiotic stress and pathogen attack (Dong et al., 2006; Rampitsch et al., 2006; Zang and Komatsu, 2007).

Cellular organization and signalling is greatly influenced by mem- bers of Ras superfamily small guanosine triphosphate (GTP)-binding proteins. In plants the superfamily is categorized into the Rho, Rab, Arf and Ran families according to their GTP-binding domain. The Rab family is by far the largest family of Ras superfamily with multiple non-clarified functions in vesicular transport and protein trafficking between differ- ent organelles via endocytotic and secretory pathways (Nielsen et al., 2008; Zhang et al., 2012). Ras-related protein Rab11D (spot 4; Table 1) exhibited an increase in abundance at 0.25 h as compared to control. At 3.25 h the abundance of this protein was lower than at 0.25 h but still higher than in the control, thus showing some adaptation

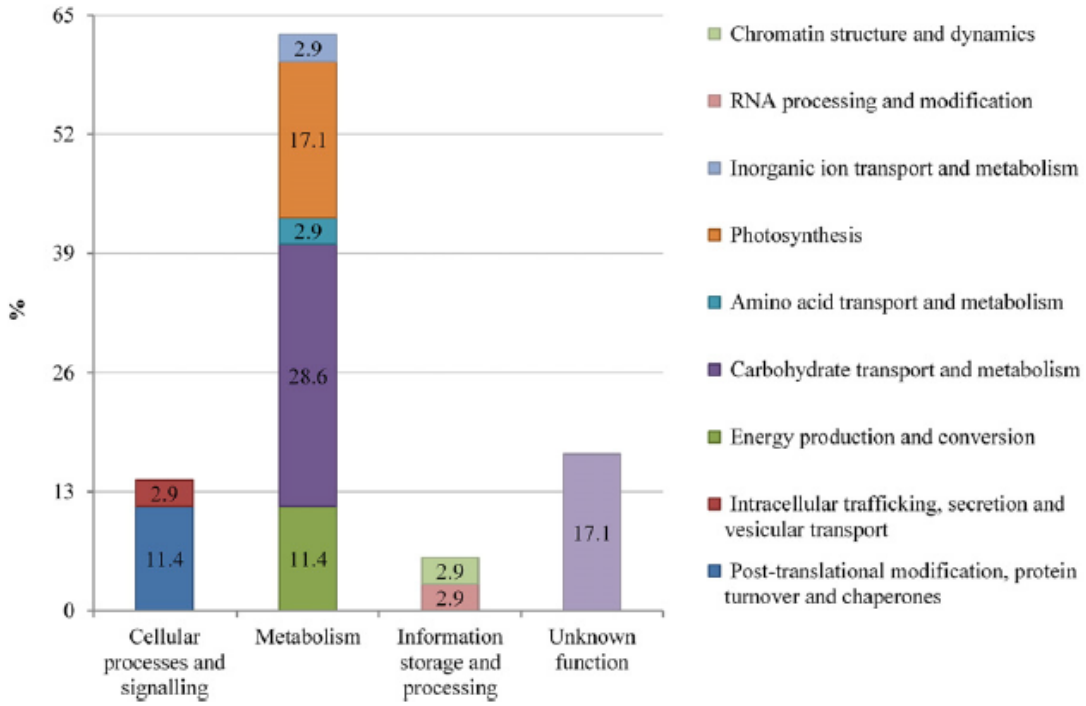

Fig. 4. Ontological classification of identified *Phragmites* sp. leaf proteins based on UniProtKB, EggNOG, KEGG databases and other reports in the literature.

Table 2
Time-dependent alterations of the proteome of *Phragmites* sp. leaves due to Acid Orange 7 (AO7). T_0: control, feeding with water; $T_{0.25\ h}$ and $T_{3.25\ h}$: 1st and 2nd pulse feeding cycles with 400 mg L^{-1} of AO7.

Time	Abundance change ($p < 0.05$)	Number of proteins	Spot ID[a]
$T_{0.25h}/T_0$	Increased	7	4, 8, 12, 17, 24, 51 and 54
	Decreased	6	9, 10, 14, 16, 20 and 32
$T_{3.25h}/T_0$	Increased	10	4, 8, 10, 12, 14, 16, 17, 24, 29 and 45
	Decreased	5	9, 20, 32, 51 and 54

[a] Consistent with the spot number of Fig. 1 and Table 1.

flexibility as observed in gene expression of Ras-related protein Rab11D in maize leaves under salt stress (Qing et al., 2009).

3.2.2. Proteins involved in energy metabolism Large amounts of ATP are required to provide sufficient energy for plant growth, development and stress response. Phragmites energy metabolism was changed under the chemical stress as suggested by the
altered abundance of two isoforms of ATPase (3 (spots 9 and 10; Table 1). At 3.25 h, the abundance ofthe mitochondrial isoform (spot 9) remained at lower levels but the abundance of plastid isoform (spot 10) showed increased levels. The same behaviour was noticed for the Hypothetical protein POPTR_0003s12000g (spot 14; Table 1). According to KEGG Orthology, this protein is classified as being involved

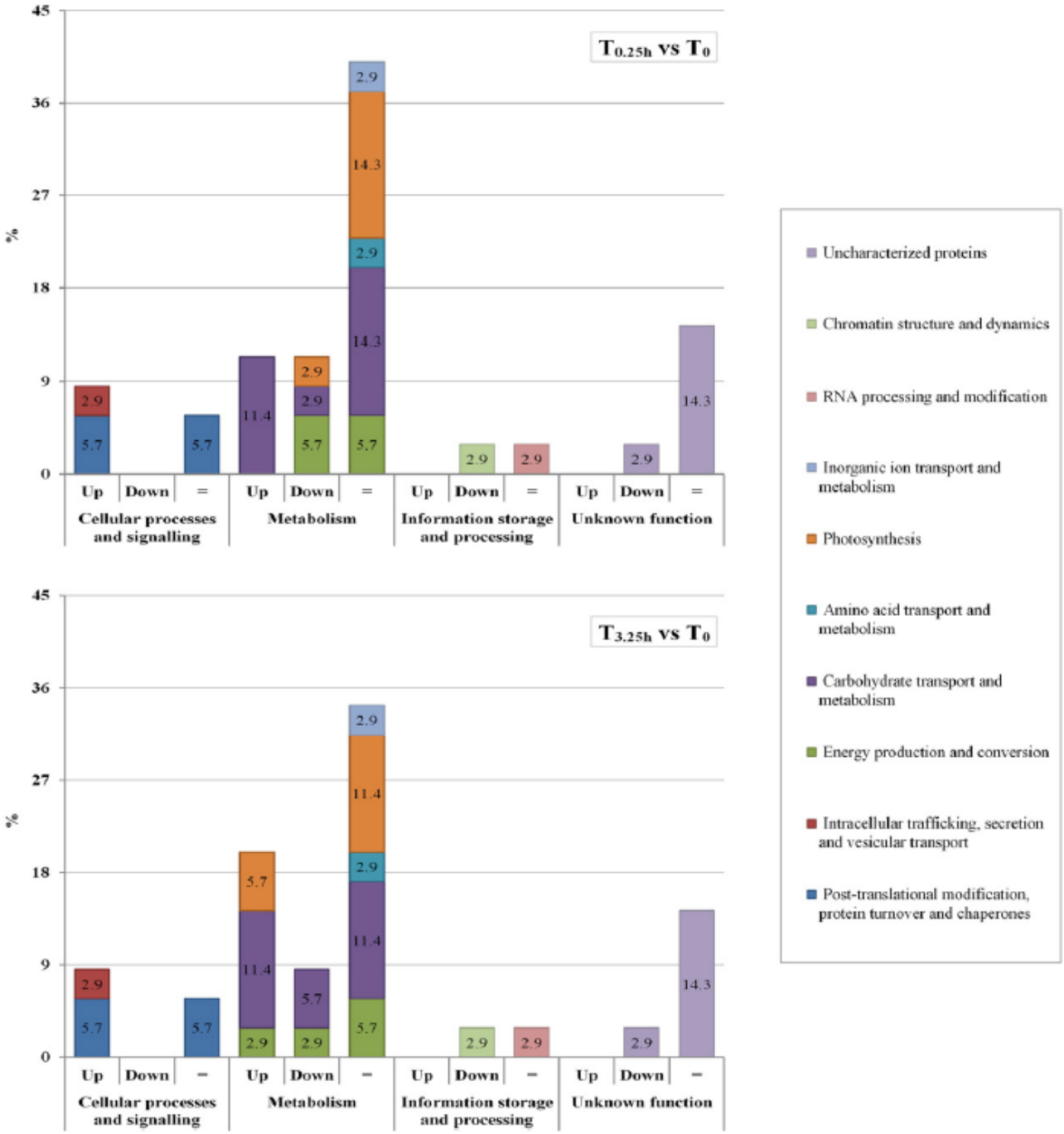

Fig. 5. Different expression levels ($p < 0.05$) and ontological classification of the identified *Phragmites* sp. leaf proteins, based on UniProtKB, EggNOG, KEGG databases and other reports in the literature. Leaves were collected from a VFCW at the end of a last water pulse (T_0) and at the end of the 1st ($T_{0.25h}$) and 2nd ($T_{3.25h}$) feeding period of AO7 (400 mg L^{-1}). Up: protein abundance increase comparatively to control; Down: protein abundance decrease comparatively to control; =: no significant difference.

in the amino sugar and nucleotide sugar metabolism. Therefore, the combined action of ATPase (3 subunits and Hypothetical protein POPTR_0003s12000g suggest that these proteins may have a protective role by providing continuously energy for normal physiological processes and, at the same time, the extra energy needed for defence mechanisms.

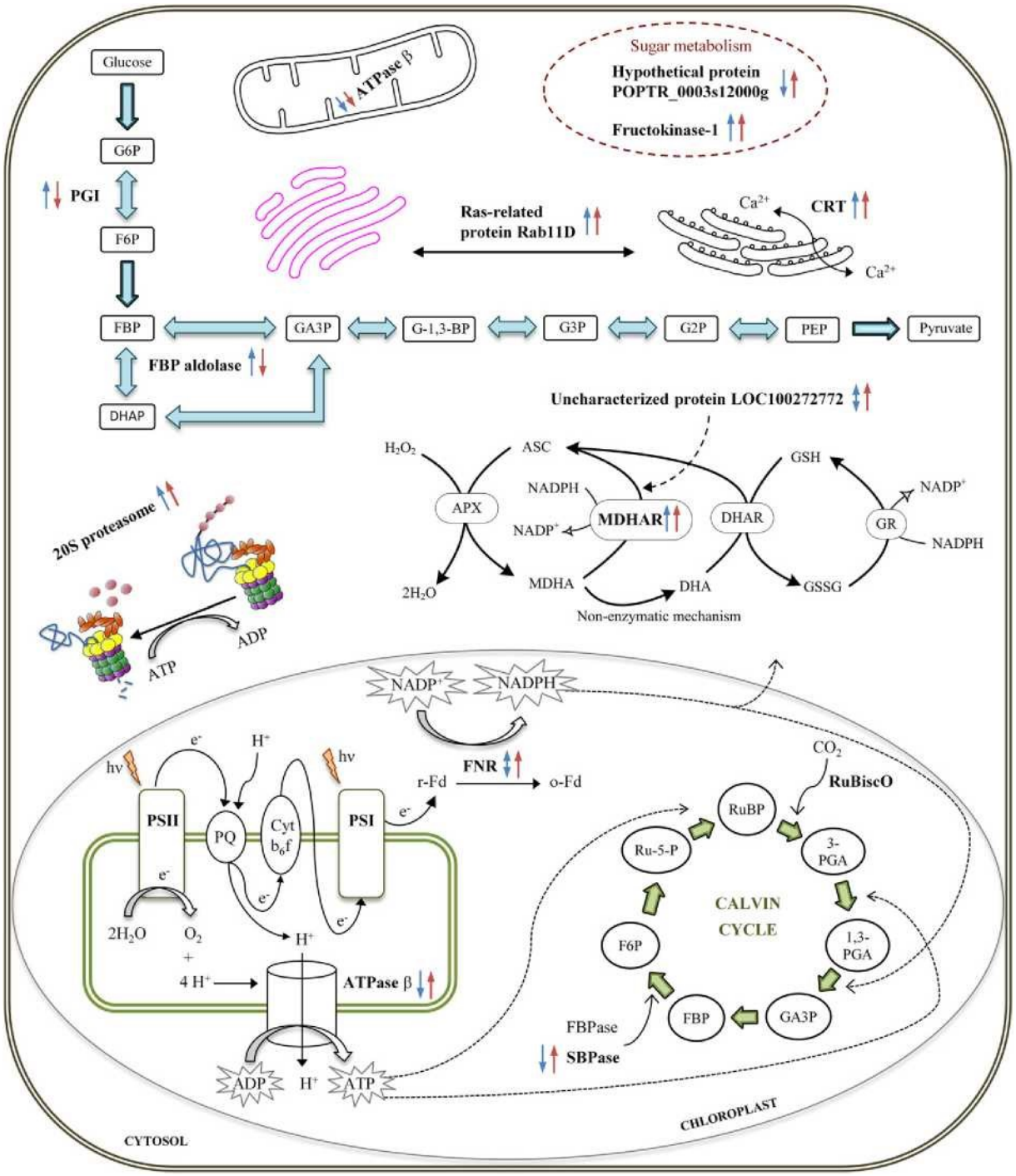

Fig. 6. Schematic representation of major chemical stress-responsive proteins of Phragmites sp. leaves. Blue (left) and red (right) arrows indicate changes in protein abundance at 0.25 h and 3.25 h (end of the 1st and 2nd feeding period of AO7 cycles), respectively; and upward arrows indicate increase, downward arrows indicate decrease and bi-arrows indicate no significantly different (p b 0.05) from the control (last water pulse). Abbreviations: 1,3-PGA, 1,3-bis phosphoglycerate; 20SP, 20S proteasome; 3-PGA, 3-phosphoglycerate; ADP, adenosine diphosphate; APX: ascorbate peroxidase; ASC: ascorbate; ATP, adenosine triphosphate; ATPase 3, adenosine triphosphate synthase beta subunit; CRT, calreticulin; Cytb6f, cytochrome b6f; DHA: dehydroascorbate; DHAP, dihydroxyacetone phosphate; DHAR: dehydroascorbate reductase; F6P, fructose-6-phosphate; FBP aldolase, fructose-bisphosphate aldolase; FBP, fructose 1,6-bisphosphate; FBPase, fructose-1,6-bisphosphatase; FNR, ferredoxin-NADP$^+$ reductase; G-1,3-BP, glycerate-1,3-bisphosphate; G2P, glycerate-2-phosphate; G3P, glycerate-3-phosphate; G6P, glucose-6-phosphate; GA3P, glyceraldehyde-3-phosphate; GR: glutathione reductase; GSH: reduced glutathione; GSSG: oxidised glutathione; MDHA: monodehydroascorbate; MDHAR: monodehydroascorbate reductase; NADP$^+$/NADPH, nicotinamide adenine dinucleotide phosphate; o-Fd, oxidised ferredoxin; PEP, phosphoenolpyruvate; PGI, phosphoglucose isomerase; PQ, plastoquinone; PSI, photosystem I; PSII, photosystem II; r-Fd, reduced ferredoxin; Ru-5-P, ribulose-5-phosphate; RuBisCO, ribulose-1,5-bisphosphate carboxylase/oxygenase; RuBP, ribulose- 1,5-bisphosphate; SBPase, sedoheptulose-1,7-bisphosphatase.

3.2.3. Photosynthesis-related proteins

An alteration between the rate of primary and secondary photosyn- thetic reactions increases the risk of ROS formation. When an imbalance in the production of ROS occurs, H2O2 may accumulate in chloroplasts and rapidly oxidise protein thiol groups leading to the inactivation of thiol-modulated Calvin cycle enzymes, such as SBPase (Foyer, 2002), Fig. 6. Once the steady state levels of H2O2 were reached (probably by their disproportionation catalysed by antioxidant enzymes like ascor- bate peroxidase (APX), peroxidase, glutathione peroxidase or catalase (Mittler et al., 2004)), a subsequent SBPase activation is expected (Raines et al., 1999) which, may be related to SPBase abundance in- crease noticed at 3.25 h. At the same time, the abundance of FNR also in- creased. In fact, this protein only presented a change in abundance after 3.25 h. FNRs are flavoenzymes, which main role in chloroplast is to ca- talyse the final step of photosynthetic electron transport, namely, the electron transfer from the ferredoxin, reduced by photosystem

I, to the oxidised form of nicotinamide adenine dinucleotide phosphate ($NADP^+$). This reaction provides the NADPH necessary for CO2 assimila- tion in the Calvin cycle and other biosynthetic and protective pathways (Fig. 6). FNR has also been suggested to confer tolerance to oxidative stress, in a combined action with flavodoxin, by maintaining proper electron distribution during oxidative stress episodes and therefore, chloroplastic redox homeostasis (Giró et al., 2011). Ferredoxin/ thioredoxin system also contributes to the redox regulation of SBPase and consequently to its activation (Raines et al., 1999). Moreover, if photosystem II is non-functional or no $NADP^+$ is available for reduction, FNR is supposed to play a role in cyclic electron transfer, generating a transmembrane pH gradient allowing ATP production (Grzyb et al., 2008). In the current work, both scenarios are possible. Further studies are needed to clarify the ultimate role of FNR in the Phragmites sp. response to the chemical stress imposed by the dye.

3.2.4. Proteins involved in carbohydrate transport and metabolism

The cytoplasmatic isozyme 1-like FBP aldolase (spot 51; Table 1) presented a 1.9-fold increase at 0.25 h. Nonetheless, at 3.25 h the pro- tein abundance presented a 0.6-fold decrease comparatively to control (0 h). In literature, there are different reports on the expression of FBP aldolase in plant leaves (Abbasi and Komatsu, 2004; Agrawal et al., 2002; Jedmowski et al., 2014; Liu et al., 2014). In this work, as in Murad et al. (2014), two other isoforms were identified (spot 61 and 62; Table 1) but without any differences in their content levels.

FBP aldolase is a key enzyme of plants metabolism, which plays a critical role in the regulation of carbon flux through carbohydrate me- tabolism. It is involved in the glycolytic pathway and reversibly cataly- ses the conversion of fructose-1,6-bisphospate to glyceraldehyde-3- phosphate and dihydroxyacetone phosphate. The cellular localization of FBP aldolase may influence the function of the protein (Jedmowski et al., 2014).

The glycolytic pathway occurs in two stages, briefly: in the 1st stage, glucose is phosphorylated twice and cleaved to form glyceraldehyde-3- phosphate; in the 2nd stage, glyceraldehyde-3-phosphate is converted to pyruvate. In the 2nd reaction of the 1st stage of glycolysis, catalysed by PGI, glucose-6-phosphate is reversibly converted to fructose-6- phosphate, that will be phosphorylated by a phosphofructokinase to form fructose-1,6-bisphospate that will be cleaved by FBP aldolase (Fig. 6). Thus, it was not surprising that FBP aldolase and PGI proteins (spot 51 and 54, respectively; Table 1) presented the same abundance variation pattern.

The overexpression of the glycolysis pathway enzymes are of utmost importance for the increase of soluble sugars accumulation, as well as for providing more energy needed for the plant under stress, and there- fore, can be an indicator of stress tolerance (Murad et al., 2014). More- over, the initial increased expression of FBP aldolase and PGI proteins may reflect the pattern of carbon flux in response to the reduction of the photosynthetic protein SBPase at 0.25 h (spot 16; Table 1) and to the high demand for the metabolic regulation in the leaves of Phragmites
caused by the dye. Seong et al. (2013) results indicated that PGI expres- sion may control antioxidant-related genes such as APX and thus, be in- volved in antioxidant metabolism. The inhibition of the glycolytic flux shifts glucose into the pentose phosphate pathway to produce NADPH, which protects against oxidative stress by providing the reducing power for antioxidant enzymes (Fernández-Cisnal et al., 2014). Proba- bly, one of the oxidoreductase proteins consuming NADPH was the up-regulated monodehydroascorbate reductase (MDHAR) (spot 12; Table 1). The Uncharacterized protein LOC100272772 (spot 45; Table 1) change in abundance at 3.25 h may also be related to ROS con- trol. According to Gene Ontology, its putative biological process is linked to hydrogen peroxide catabolic process. Moreover, and according to KEGG Orthology, this protein is defined as a MDHAR. This protein catal- yses the conversion of the monodehydroascorbate to ascorbate oxidiz- ing NAPDH (Fig. 6). Dismutation of H2O2 to H2O by APX occurs by oxidation of ascorbate. A previous study (Carias et al., 2008) reported an increase in leaves APX activity after Phragmites has been exposed to low concentrations of AO7. Moreover, early changes (at 0.25 h) in photosynthetic pigments content (depletion) and in APX activity (in- crease) in Phragmites sp. leaf soluble proteins were verified in response to exposure to a di-azo dye contaminated effluent (Ferreira et al., 2014). Additionally and assuming that photosynthesis inhibition took place under chemical stress imposed by AO7, the plant energy and carbon re- quirements need to be derived from stored carbohydrates. This hypoth- esis is supported by the increased content of FBP aldolase and PGI proteins, and of fructokinase-1 (spot 17; Table 1), which catalyses the key step of fructose phosphorylation in plants.

4. Conclusions

After a perturbation, the proteome is generally altered in order to adapt the cell to the new environmental condition. In this study, the comparison of the protein abundance profile of plant leaf samples be- fore and after the plants irrigation with AO7 at 400 mg L^{-1} allowed for the identification of proteins that were affected.

Overall, this comparative proteomic analysis led to the identification of 35 proteins, 15 of them showing a

different abundance in relation to control within a 3.25 h period. AO7 has a prompt effect on the content of proteins of Phragmites sp. leaf photosynthetic apparatus and on proteins related to energy production and conversion and to carbohydrate trans- port and metabolism. Signalling to the oxidative stress imposed by the dye was also rapidly activated. The obtained results are a contribution into the analysis and further establishment of Phragmites sp. phytoremediation mechanisms. Moreover, it is important to highlight that carbohydrate metabolism boosted the energy flows due to photo- synthesis inhibition. Thus, significative changes in the photosynthetic apparatus should be correlated with all the other prompt response mechanisms to assess plant species sensitivity to the azo dyes prior phytoremediation implementation.

Supplementary data to this article can be found online at http://dx.doi.org/10.1016/j.scitotenv.2016.08.169.

Acknowledgements

The authors acknowledge financial support from the Fundação para a Ciência e a Tecnologia (projects PTDC/AMB/67641/2006, PTDC/AAC- AMB/112032/2009 and a PhD scholarship SFRH/BD/38805/2007 to CRR) and from CUF-Químicos Industriais, S.A. (industrial partner). Funding received by IBB-Institute for Bioengineering and Biosciences from Programa Operacional Regional de Lisboa 2020 (N. 007317) and by CERENA is acknowledged as well.

References

Abbasi, F.M., Komatsu, S., 2004. A proteomic approach to analyze salt-responsive proteins in rice leaf sheath. Proteomics 4, 2072-2081.

Agrawal, G.K., Rakwal, R., Yonekura, M., Kubo, A., Saji, H., 2002. Proteome analysis of dif- ferentially displayed proteins as a tool for investigating ozone stress in rice (Oryza sativa L.) seedlings. Proteomics 2,947-959.

Banat, I.M., Nigam, P., Singh, D., Marchant, R., 1996. Microbial decolorization of textile- dyecontaining effluents: a review. Bioresour. Technol. 58, 217-227.

Barac, T., Taghavi, S., Borremans, B., Provoost, A., Oeyen, L., Colpaert, J.V., et al., 2004. Engineered endophytic bacteria improve phytoremediation of water-soluble, volatile, organic pollutants. Nat. Biotechnol. 22, 583-588.

Bhaskar, M., Gnanamani, A., Ganeshjeevan, R.J., Chandrasekar, R., Sadulla, S., Radhakrishnan, G., 2003. Analyses of carcinogenic aromatic amines released from harmful azo colorants by Streptomyces SP. SS07. J. Chromatogr. A. 1018, 117-123.

Carias, C.C., Novais, J.M., Martins-Dias, S., 2008. Are Phragmites australis enzymes involved in the degradation of the textile azo dye acid orange 7? Bioresour. Technol. 99, 243-251.

Chung, K.-T., Stevens, S.E., Cerniglia, C.E., 1992. The reduction of azo dyes by the intestinal microflora. Crit. Rev. Microbiol. 18, 175-190.

Collins, C., Martin, I., Fryer, M., 2006. Evaluation of models for predicting plant uptake of chemicals from soil. Science Report - SC050021/SR 1. Environment Agency, Bristol.

Cui, S.X., Hu, J., Yang, B., Shi, L., Huang, F., Tsai, S.N., et al., 2009. Proteomic characterization of Phragmites communis in ecotypes of swamp and desert dune. Proteomics 9, 3950-3967.

Davies, L.C., Pedro, I.S., Novais, J.M., Martins-Dias, S., 2006. Aerobic degradation of acid or- ange 7 in a vertical-flow constructed wetland. Water Res. 40, 2055-2063.

Davies, L.C., Cabrita, G.J.M., Ferreira, R.A., Carias, C.C., Novais, J.M., Martins-Dias, S., 2009. Integrated study of the role of Phragmites australis in azo-dye treatment in a con- structed wetland: from pilot to molecular scale. Ecol. Eng. 35, 961-970.

Davies, L.C., Roma-Rodrigues, C., Sá-Correia, I., Novais, J.M., Martins-Dias, S., 2010. Proteo- mics applied to phytoremediation. In: Marko-Varga, G., Simões, T. (Eds.), 2010: A Pro- teomics Odyssey Towards Next Decades. Apotekarsocieteten, Estoril, Portugal, pp. 255-256.

Demidchik, V., 2015. Mechanisms of oxidative stress in plants: from classical chemistry to cell biology. Environ. Exp. Bot. 109, 212-228.

Dong, W., Nowara, D., Schweizer, P., 2006. Protein polyubiquitination plays a role in basal host resistance of barley. Plant Cell 18, 3321-3331.

Fernández-Cisnal, R., Alhama, J., Abril, N., Pueyo, C., López-Barea, J., 2014. Redox proteo- mics as biomarker for assessing the biological effects of contaminants in crayfish from Donana National Park. Sci. Total Environ. 490,121-133.

Ferreira, R.A., Duarte, J.G., Vergine, P., Antunes, C.D., Freire, F., Martins-Dias, S., 2014. Phragmites sp. physiological changes in a constructed wetland treating an effluent contaminated with a diazo dye (DR81). Environ. Sci. Pollut. R. 21, 9626-9643.

Foyer, C.H., 2002. The contribution of photosynthetic oxygen metabolism to oxidative stress in plants. In:

Inzé, D., Montagu, M.V. (Eds.), Oxidative Stress in Plants. Taylor & Francis, London, pp. 40-84.
Garg, G., Yadav, S., Ruchi, Y.G., 2015. Key roles of calreticulin and calnexin proteins in plant perception under stress conditions: a review. Adv. Life Sci. 5, 18-25.
Ghaly, A.E., Ananthashankar, R., Alhattab, M., Ramakrishnan, V.V., 2014. Production, char- acterization and treatment of textile effluents: a critical review. J. Chem. Eng. Process. Technol. 5, 1 -18.
Giró, M., Ceccoli, R.D., Poli, H.O., Carrillo, N., Lodeyro, A.F., 2011. An in vivo system involv- ing co-expression of cyanobacterial flavodoxin and ferredoxin-NADP(+) reductase confers increased tolerance to oxidative stress in plants. FEBS Open Bio. 1, 7-13.
Grzyb, J., Malec, P., Rumak, I., Garstka, M., Strzalka, K., 2008. Two isoforms of ferredoxin: NADP+ oxidoreductase from wheat leaves: purification and initial biochemical char- acterization. Photosynth. Res. 96, 99-112.
Gupta, D., Tuteja, N., 2011. Chaperones and foldases in endoplasmic reticulum stress sig- naling in plants. Plant Signal. Behav. 6, 232-236.
Haberl, R., Grego, S., Langergraber, G., Kadlec, R.H., Cicalini, A.-R., Martins Dias, S., et al., 2003. Constructed wetlands for the treatment of organic pollutants. J. Soil Sediment. 3, 109-124.
Heilmann, I., Shin, J., Huang, J., Perera, I.Y., Davies, E., 2001. Transient dissociation ofpoly- ribosomes and concurrent recruitment of calreticulin and calmodulin transcripts in gravistimulated maize pulvini. Plant Physiol. 127, 1193-1203.
Hinsinger, P., Bengough, A.G., Vetterlein, D., Young, I., 2009. Rhizosphere: biophysics, bio- geochemistry and ecological relevance. Plant Soil 321, 117-152.
Jedmowski, C., Ashoub, A., Beckhaus, T., Berberich, T., Karas, M., et al., 2014. Comparative analysis of Sorghum bicolor proteome in response to drought stress and following re- covery. Int. J. Proteomics 2014, 1-10 Br.
Komatsu, S., Yang, G., Khan, M., Onodera, H., Toki, S., Yamaguchi, M., 2007. Over- expression of calcium-dependent protein kinase 13 and calreticulin interacting pro- tein 1 confers cold tolerance on rice plants. Mol. Gen. Genomics. 277, 713-723.
Kosová, K., Vítámvás, P., Prásil, I.T., Renaut,J., 2011. Plant proteome changes under abiotic stress - contribution of proteomics studies to understanding plant stress response. J. Proteomics 74, 1301-1322.
Liu, G.-T., Ma, L., Duan, W., Wang, B.-C., Li, J.-H., Xu, H.-G., et al., 2014. Differential proteo- mic analysis ofgrapevine leaves by iTRAQ reveals responses to heat stress and subse- quent recovery. BMC Plant Biol. 14, 1 -17.
Madeira, A., Santos, P.M., Coutinho, C.P., Pinto-de-Oliveira, A., Sá-Correia, I., 2011. Quanti- tative proteomics (2-D DIGE) reveals molecular strategies employed by Burkholderia cenocepacia to adapt to the airways of cystic fibrosis patients under antimicrobial therapy. Proteomics 11, 1313-1328.
Mittler, R., Vanderauwera, S., Gollery, M., Van Breusegem, F., 2004. Reactive oxygen gene network of plants. Trends Plant Sci. 9, 490-498.
Murad, A.M., Molinari, H.B.C., Magalhães, B.S., Franco, A.C., Takahashi, F.S.C., de Oliveira, N.G., et al., 2014. Physiological and proteomic analyses of Saccharum spp. grown under salt stress. Plos One 9, e98463.
Nielsen,E., Cheung, A.Y., Ueda, T., 2008. The regulatory RABand ARF GTPases for vesicular trafficking. Plant Physiol. 147, 1516-1526.
Qing, D.J., Lu, H.F., Li, N., Dong, H.T., Dong, D.F., Li, Y.Z., 2009. Comparative profiles ofgene expression in leaves and roots of maize seedlings under conditions of salt stress and the removal of salt stress. Plant Cell Physiol. 50, 889-903.
Qiu, Y., Xi, J., Du, L., Poovaiah, B.W., 2012. The function of calreticulin in plant immunity: new discoveries for an old protein. Plant Signal. Behav. 7, 907-910.
Raines, C.A., Lloyd, J.C., Dyer, T.A., 1999. New insights into the structure and function of sedoheptulose-1,7-bisphosphatase; an important but neglected Calvin cycle enzyme. J. Exp. Bot. 50, 1 -8.
Rampitsch, C., Bykova, N.V., McCallum, B., Beimcik, E., Ens, W., 2006. Analysis ofthe wheat and Puccinia triticina (leafrust) proteomes during a susceptible host-pathogen inter- action. Proteomics 6, 1897-1907.
Roma-Rodrigues, C., Santos, P.M., Benndorf, D., Rapp, E., Sá-Correia, I., 2010. Response of Pseudomonas putida KT2440 to phenol at the level of membrane proteome. J. Proteomics 73, 1461-1478.
Sanromán, M.A., Pazos, M., Ricart, M.T., Cameselle, C., 2004. Electrochemical decolourisation of structurally different dyes. Chemosphere 57, 233-239.
Santos, P.M., Sa-Correia, I., 2009. Adaptation to beta-myrcene catabolism in Pseudomonas sp. M1: an expression proteomics analysis. Proteomics 9, 5101-5111.
Santos, P.M., Benndorf, D., Sa-Correia, I., 2004. Insights into Pseudomonas putida KT2440 response to phenol-induced stress by quantitative proteomics. Proteomics 4, 2640-2652.
Schuerenbeg, M., Luebbert, C., Eickhoff, H., Kalkum, M., Lehrach, H., Nordhoff, E., 2000. Prestructured

MALDI-MS sample supports. Anal. Chem. 72, 3436-3442.
Schwitzguébel, J.-P., Page, V., Martins-Dias, S., Davies, L., Vasilyeva, G., Strijakova, E., 2011. Using plants to remove foreign compounds from contaminated water and soil. In: Schroder, P., Collins, C.D. (Eds.), Organic Xenobiotics and Plants 8. Springer Netherlands, pp. 149-189.
Seong, E.S., Yoo, J.H., Lee, J.G., Kim, H.Y., Hwang, I.S., Heo, K., et al., 2013. Transient overex- pression ofthe Miscanthus sinensis glucose-6-phosphate isomerase gene (MsGPI) in Nicotiana benthamiana enhances expression of genes related to antioxidant metabo- lism. Plant Omics 6, 408-414.
Sharma, A., Isogai, M., Yamamoto, T., Sakaguchi, K., Hashimoto, J., Komatsu, S., 2004. A novel interaction between calreticulin and ubiquitin-like nuclear protein in rice. Plant Cell Physiol. 45, 684-692.
Shevchenko, A., Tomas, H., Havlis, J., Olsen, J.V., Mann, M., 2006. In-gel digestion for mass spectrometric characterization of proteins and proteomes. Nat. Protoc. 1, 2856-2860.
Suckau, D., Resemann, A., Schuerenberg, M., Hufnagel, P., Franzen, J., Holle, A., 2003. A novel MALDI LIFT-TOF/TOF mass spectrometer for proteomics. Anal. Bioanal. Chem. 376, 952-965.
Verkleij,J.A.C., Golan-Goldhirsh, A., Antosiewisz, D.M., Schwitzguébel, J.-P., Schroder, P., 2009. Dualities in plant tolerance to pollutants and their uptake and translocation to the upper plant parts. Environ. Exp. Bot. 67, 10-22.
Wu, H., Zhang, J., Ngo, H.H., Guo, W., Hu, Z., Liang, S., et al., 2015. A review on the sustain- ability of constructed wetlands for wastewater treatment: design and operation. Bioresour. Technol. 175, 594-601.
Yan, S., Du, X., Wu, F., Li, L., Li, C., Meng, Z., 2014. Proteomics insights into the basis of in- terspecific facilitation for maize (Zea mays) in faba bean (Vicia faba)/maize intercropping. J. Proteomics 109, 111 - 124.
Zang, X., Komatsu, S., 2007. A proteomics approach for identifying osmotic-stress-related proteins in rice. Phytochemistry 68, 426-437.
Zhang, X., Li, J., Liu, A., Zou, J., Zhou, X., Xiang, J., et al., 2012. Expression profile in rice panicle: insights into heat response mechanism at reproductive stage. PLoS One 7, e49652.

This is a post-peer-review version of an article published in Science of the Total Environment, 2016 following peer review. The version of record Ferreira, R., Roma-Rodrigues, C., Davies, L., Sá-Correia, I. & Martins-Dias, S. (2016). A quantitative proteomic approach to highlight Phragmites sp. adaptation mechanisms to chemical stress induced by a textile dyeing pollutant. Science of the Total Environment, 573, 788-798. http://dx.doi.org/10.1016/j.scitotenv.2016.08.169